Available online at www.sciencedirect.com

ScienceDirect

*Mendeleev Commun.*, 2023, **33**, 701–704

Mendeleev Communications

# New electron-deficient 2,1,3-benzothiadiazole-cored donor–acceptor compounds: synthesis, photophysical and electroluminescent properties

**Pavel S. Gribanov,[a] Dmitry A. Loginov,[a,b] Dmitry A. Lypenko,[c] Artem V. Dmitriev,[c] Sergey D. Tokarev,[a] Alexey E. Aleksandrov,[c] Alexey R. Tameev,[c] Andrey Yu. Chernyadyev[c] and Sergey N. Osipov*[a]**

[a] *A. N. Nesmeyanov Institute of Organoelement Compounds, Russian Academy of Sciences, 119334 Moscow, Russian Federation. E-mail: osipov@ineos.ac.ru*
[b] *G. V. Plekhanov Russian University of Economics, 117997 Moscow, Russian Federation*
[c] *A. N. Frumkin Institute of Physical Chemistry and Electrochemistry, Russian Academy of Sciences, 119071 Moscow, Russian Federation*

DOI: 10.1016/j.mencom.2023.09.035

**Three new 2,1,3-benzothiadiazole-containing luminophores with different electron deficiency of acceptor block have been prepared *via* the Pd-catalyzed Suzuki cross-coupling and nucleophilic fluorine substitution with cyano group. Photophysical and electroluminescent properties of the compounds obtained were investigated to estimate their potential for optoelectronic applications. The introduction of two fluorine atoms in the benzothiadiazole moiety leads to the hypsochromic shift of the electroluminescent emission, whereas the incorporation of two cyano groups shifts it into the long-wave region. All synthesized compounds were used as emissive layers in OLED devises.**

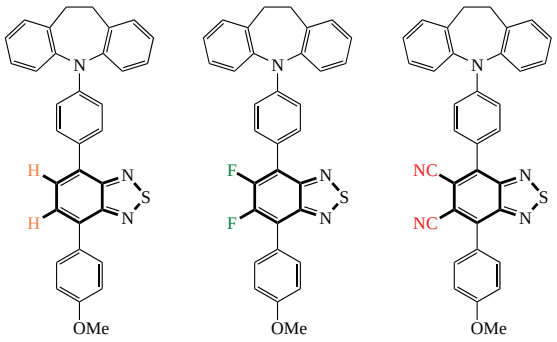


*Keywords*: luminophore, benzothiadiazole, cross-coupling, luminescence, OLED.

In recent years, a considerable attention in the field of organic and photochemistry has been focused on the creation of innovative photoactive materials aimed at solving a number of important practical goals. The development of such materials involves the search for new π-conjugated donor–acceptor (D–A) systems and a detailed study of their photophysical and electronic properties. In this context, acceptor building blocks based on the strong electron deficient 2,1,3-benzothiadiazole (Bz) have attracted much attention in preparing optoelectronic devices[1] with improved characteristics, such as organic light emitting diodes (OLEDs),[2] field effect transistors,[3] solar cells,[4] luminescent solar concentrators[5] and as fluorescent tags for molecular and cellular imaging.[6]

The incorporation of the additional electron-withdrawing substituents into Bz moiety to increase its electron affinity is often used to fine-tune the required photophysical properties. Recently, 5,6-difluoro-2,1,3-benzothiadiazole (BzF) has been utilized to lower the HOMO and LUMO levels of conjugated D–A molecules. In this regard, many BzF-based compounds have been synthesized and applied for the construction of high-performance optoelectronic materials.[7]

Among various electron-withdrawing functionalities, cyano group (CN) is the strongest one and has been widely employed to lower LUMO energy level of small molecules, *e.g.*, cyano-functionalized air stable *n*-type rylene diimides and quinonoid fused *n*-type semiconductors.[8] The CN group has an exceptional large dipole moment,[9] which can favor charge separation in films.[10] As a result, dicyano-2,1,3-benzothiadiazole-based molecules (BzCNs) have been recently investigated in the context of their optoelectronic properties exhibiting extremely low LUMO levels and unipolar electron transport properties. In 2020, Promarak used extremely strong electron-deficient 5,6-dicyano-2,1,3-benzothiadiazole (BzCN) as an acceptor core for constructing an efficient NIR thermally activated delayed fluorescence (TADF) fluorophores.[11] Therefore, the development of new Bz-based D–A molecules and investigation of their photophysical characteristics are of great current interest. In continuation of our research in the field,[12] and inspired by Promarak work, here we wish to disclose an efficient synthesis of three new unsymmetrically substituted Bz-containing luminophores with different electron deficiency of acceptor block, their photophysical properties and the working characteristics of OLEDs fabricated on their basis as well.

A synthetic route to the Bz-containing compounds DABzH and DABzF included Pd-catalyzed Suzuki cross-coupling reactions of readily available 4-bromo-substituted derivatives **1**[12(*a*)] and **2**[12(*d*)] with 5-[4-(4,4,5,5-tetramethyl-1,3,2-dioxaborolan-2-yl)phenyl]-10,11-dihydro-5*H*-dibenzo[*b*,*f*]azepine **3**.[12(*c*)] The both reactions were accomplished under reflux in a mixture of dioxane/water in the presence of catalytic amounts of $PdCl_2(PPh_3)_2$ and excess of $NaHCO_3$ to afford the corresponding new unsymmetrical D–A molecules DABzH and DABzF in good and excellent yields. Subsequent nucleophilic substitution of two fluorine atoms of DABzF with cyano groups was performed by treatment with sevenfold excess of potassium cyanide in DMF in the presence of 18-crown-6 ether (10 mol%) at 50 °C yielding the desired dicyano containing product DABzCN (Scheme 1). All compounds obtained were putified by flash chromatography followed by sublimation (200–220 °C/

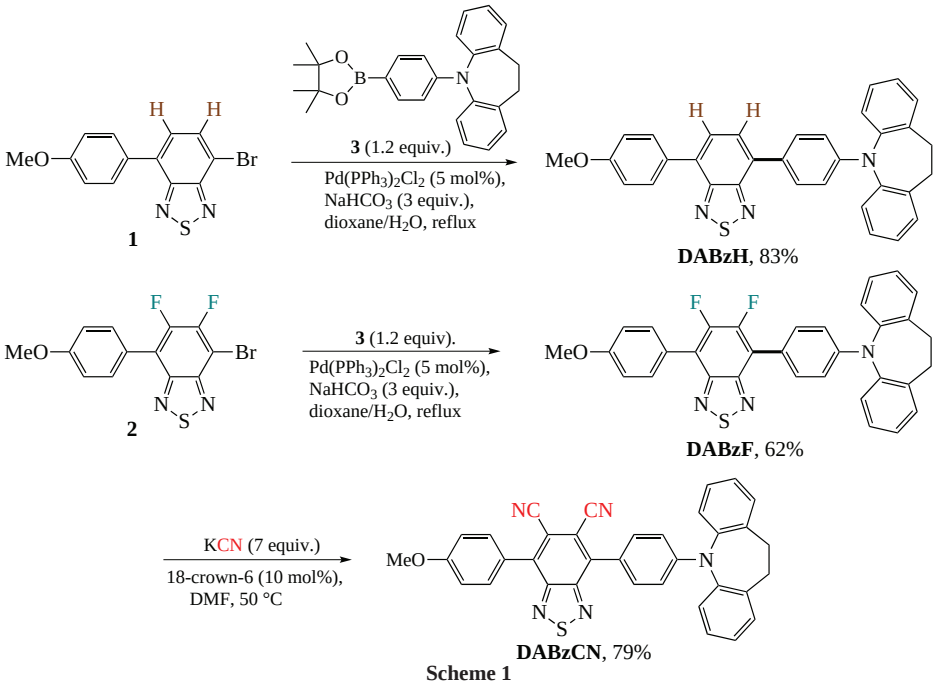


**Scheme 1**

0.1 Torr). Their structures were characterized using $^{1}H$, $^{19}F$, $^{13}C$ NMR, and HRMS (see Online Supplementary Materials).

The redox potentials of DABzH, DABzF and DABzCN were investigated by cyclic voltammetry (CVA) in $Bu_4NPF_6/CH_2Cl_2$ on a 2 mm glassy carbon electrode (see Online Supplementary Materials, Figures S1–S3). All studied compounds exhibit reversible oxidations, namely, $E_{1/2OX}$ values for DABzH, DABzF and DABzCN are located at about 1.0, 1.1 and 1.2 V (*vs.* Ag/AgCl), respectively. This shows that attempts to increase the electron withdrawing power of the benzothiadiazole fragment by introducing fluorine atoms or CN-groups do have an effect on the electron density localization in the molecule. The HOMO energy decreases despite the absence of changes in the donor part of the molecule. In the cathodic region, the reversible reduction occurs at about –1.5 V for DABzH and DABzF, while for DABzCN at –1.0 V (*vs.* Ag/AgCl). Thus, the introduction of CN-groups significantly increases the acceptor strength of benzothiadiazole, but the fluorine atoms do not show any noticeable effect. Energies of frontier molecular orbitals calculated from the redox potentials are given in Table 1. The experimental values of HOMO–LUMO gap ($E_g$) fully correlate with blue shift of emission bands for DABzF and red shift for DABzCN (Figures 1, 2).

**Table 1** FMO's energies obtained from CVA.

| Compound | HOMO/eV | LUMO/eV | $E_g$[a]/eV |
|---|---|---|---|
| DABzH | –5.30 | –2.81 | 2.49 |
| DABzF | –5.44 | –2.87 | 2.57 |
| DABzCN | –5.59 | –3.39 | 2.20 |

[a] $E_g$ is energy difference HOMO–LUMO gap, which was calculated as $E_g$ = HOMO – LUMO.

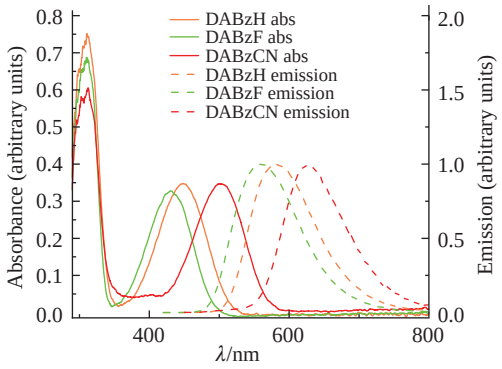


**Figure 1** Optical spectra of DABzH, DABzF, DABzCN in *m*-xylene (concentration $10^{-5}$ M, optical length 1 cm, $\lambda_{ex}$ = 375–400 nm) at room temperature.

The luminescent properties of DABzH, DABzF, DABzCN were evaluated in solutions of *m*-xylene as well as in solid films obtained by the thermal vacuum evaporation (TVE) method on a quartz plate. Their photoluminescence spectra in *m*-xylene exhibit wide bands that are mirror-symmetrical to the wide charge transfer bands in the UV/VIS-spectra (Table 2 and Figure 1).

**Table 2** Absorption and emission characteristics of DABzH, DABzF and DABzCN at 298 K.[a]

| Substance | $\lambda^{abs}_{max}$ 298 K/nm | $\lambda^{PL}_{max}$ 298 K/nm (air) | $\varphi^{PL}$ 298 K (%) (air) |
|---|---|---|---|
| DABzH | 451 | 584 | 56 |
| DABzF | 434 | 558 | 53.2 |
| DABzCN | 504 | 626 | 34.3 |

[a] Absorption ($\lambda^{abs}_{max}$) and emission ($\lambda^{PL}_{max}$ – for photoluminescence) maxima, photoluminescence total quantum yield in integrating sphere ($\varphi^{PL}$), $\lambda$ excitation for luminescence – 375–400 nm; measured in *m*-xylene.

The photoluminescence quantum yields for dyes DABzH, DABzF, DABzCN in solid films, obtained by TVE method with matrixes on a quartz plate, proved to be very close to the corresponding values measured in *m*-xylene solutions, which may indicate a similar nature of the microenvironment of dye molecules in the matrix and in the *m*-xylene solution. In films, the spectra of compounds have a shape similar to that of the spectra in the *m*-xylene solution, but are bathochromically shifted in the solid (Table 3).

Electroluminescent properties of DABzH, DABzF, DABzCN were studied in OLED structures ITO/TAPC (60 nm)/dye (5–20 wt%):mCP (30 nm)/TPYMB (30 nm)/LiF (1 nm)/Al (80 nm), which were similar to those studied in our previous work.[12(b)] Here TAPC denotes 1,1-bis[4-(di-*p*-tolylamino)-phenyl]cyclohexane and serves as a hole transport layer (HTL), 3TPYMB denotes tris[2,4,6-trimethyl-3-(pyridin-3-yl)phenyl]-borane and is an electronic transport layer (ETL), ITO is the

**Table 3** Emission maxima and photoluminescence total quantum yield measured in integrating sphere in film (in mCP and CBP matrix, 15 wt%) at 298 K.

| Compound | $\lambda^{em}_{max}$, matrix CBP/nm | QY (%) | $\lambda^{em}_{max}$, matrix mCP/nm | QY (%) |
|---|---|---|---|---|
| DABzH | 595 | 52 | 599 | 57 |
| DABzF | 568 | 46 | 572 | 52 |
| DABzCN | 654 | 36 | 662 | 39 |

anode and LiF/Al is the cathode. A light emitting layer (EML) was formed by co-deposition of the dye and a host material. Two compounds, 4,4′-di(*N*-carbazolyl)-1,1′-biphenyl (CBP) and 1,3-di(*N*-carbazolyl)benzene (mCP), were used as the matrix materials in the EML. The former is one of the most widely used host materials for efficient fluorescent and phosphorescent OLEDs and possesses high hole mobility,[13] the latter is a conventional wide gap material for fabrication of efficient electrophosphorescent light emitting diodes with delayed fluorescence (TADF).[14] The studied OLEDs with an EML based on the mCP matrix showed electrical characteristics (maximum current efficiency, maximum brightness, switch-on voltage) higher compared to devices with the EML based on the CBP. In this regard, composites with a dye content in the mCP matrix from 5 to 20% were investigated and optimal characteristics were obtained for OLEDs with a dye content of 15% in the EML (Table 4).

In the studied composites, the EL bands are located in the entire visible and near-IR ranges of the spectrum, and their maxima are shifted by 5–20 nm towards the short-wavelength region relative to the corresponding photoluminescence bands of solid films (see Table 3). The color of the OLED radiation varies from yellow-green (with a maximum EL at 556 nm) for DABzF:mCP to orange (592 nm) for DABzH:mCP and red (644 nm) for DABzCN:mCP (Figure 2).

Fluorinated groups in the benzothiadiazole moiety of DABzF shift the maximum EL by 36 nm to the short-wavelength region, and the introduction of cyano groups in DABzCN shifts the maximum EL by 52 nm to the long-wavelength region of the spectrum relative to the unsubstituted DABzH. This is due to the strong influence of electron acceptor substituents on the position of the LUMO and HOMO energy levels. The points corresponding to the chromaticity of the radiation of the studied OLEDs lie on the border of the locus, which indicates the color saturation.

OLED based on the mCP:DABzH composite shows a maximum brightness of 7860 cd m$^{-2}$ at a voltage of 17 V (see Table 4). In the mCP composites, the dye DABzH exhibits a greater quantum yield of PL compared to the rest dyes DABzF and DABzCN (see Table 3). However, an OLED based on the mCP:DABzH composite demonstrates the current efficiency and external quantum efficiency of 2.84 cd A$^{-1}$ and 1.1%, respectively, lower than those for a device based on the mCP:DABzF composite (3.74 cd A$^{-1}$ and 1.92%). This is due to the low current density in the mCP:DABzF OLED compared to other diodes. It is worth noting that, despite the PL efficiency of the DABzCN:mCP composite is no more than 1.5 times lower compared to the DABzH and DABzF based composites, the current efficiency of the DABzCN based OLED is 4 and 5 times lower than that of the DABzH and DABzF based OLEDs, respectively (see Table 4).

It is obvious that the observed features of the studied OLEDs are related to the injection and transport of charge carriers; therefore, the mobility of charge carriers in dye:mCP composites were also investigated. The mobility of charge carriers in the studied composites (Table 5) is an order of magnitude lower than that in composites with dyes of a similar structure,[12(b)] but having a carbazole fragment instead of a 10,11-dihydro-5*H*-dibenz[*b*,*f*]-azepine. Using the conventional time-of-flight (TOF) technique,[15] it has been shown that the mobility of charge carriers is significantly lower for a compound with an 10,11-dihydro-5*H*-dibenz[*b*,*f*]azepine fragment compared to a compound with a carbazole fragment.

Current–voltage (*J*–*V*) characteristics of the investigated OLEDs [Figure 3(*a*)] obey the power law $J \sim U^m$ with the change in the exponent *m* from 2 (at $U < 3$ V) to 5 (at $U > 6$ V) and a steep increase in current with an increase in voltage between 3 V and 6 V. There is no suitable analytical equation for estimating mobility from *J*–*V* exponential curves with these exponent values.[16] The *J*–*V* curves show that the injection current in OLEDs with the DABzH and DABzCN is noticeably higher than that in OLED with DABzF. Yet, the brightness of the OLED based on DABzCN is much lower than in the OLEDs based on DABzH and even DABzF [Figure 3(*b*)]. We explain this by the

**Table 4** EL characteristics of the studied OLEDs with different light-emitting layers.

| Light-emitting layer | $U_{on}$/V | Max. brightness/cd m$^{-2}$ | Max. efficiency | | CIE | | $\lambda_{max}$ EL/nm |
|---|---|---|---|---|---|---|---|
| | | | current /cd A$^{-1}$ | EQE (%) | *x* | *y* | |
| DABzH:mCP | 3.8 | 7860 | 2.84 | 1.10 | 0.549 | 0.441 | 592 |
| DABzF:mCP | 5.4 | 5840 | 3.74 | 1.92 | 0.427 | 0.545 | 556 |
| DABzCN:mCP | 5.7 | 1692 | 0.71 | 0.76 | 0.653 | 0.341 | 644 |

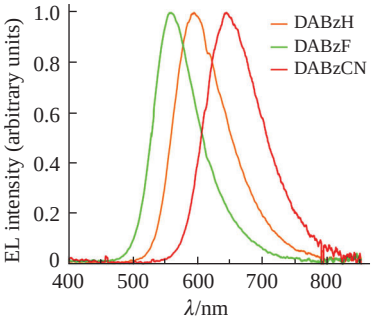


**Figure 2** EL spectra of the studied OLEDs.

**Table 5** LUMO–HOMO levels (eV) and charge carrier mobility (cm$^2$ V$^{-1}$ s$^{-1}$).

| Material | LUMO | Electron mobility | HOMO | Hole mobility |
|---|---|---|---|---|
| DABzH:mCP | –2.81 | $5.0 \times 10^{-5}$ | –5.30 | $3.0 \times 10^{-5}$ |
| DABzF:mCP | –2.87 | $2.6 \times 10^{-5}$ | –5.44 | $5.3 \times 10^{-5}$ |
| DABzCN:mCP | –3.39 | $2.9 \times 10^{-5}$ | –5.59 | $3.9 \times 10^{-5}$ |

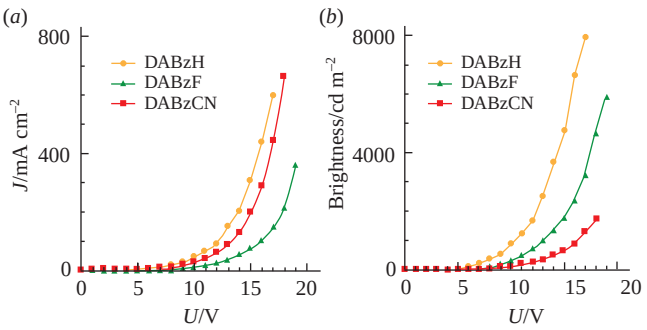


**Figure 3** (*a*) Current–voltage dependence and (*b*) voltage–brightness characteristics of the OLEDs based on EML with the DABzH, DABzF, DABzCN/mCP composites.

fact that the injected electrons and holes transport in the mCP mainly, and the dye molecules act as traps for them (see Table 5). Whereas the traps of holes in mCP/DABzCN are shallow, the time of capture of holes and the probability of their recombination with electrons in mCP/DABzCN is less than those in mCP/DABzH and mCP/DABzF. The relatively high current in the mCP/DABzCN based OLED is associated with the transport of injected charge carriers that avoided recombination. This is also reflected in the brightness of the radiation [see Table 4 and Figure 3(*b*)] of the mCP/DABzCN based OLED.

In summary, we have elaborated an efficient synthesis of three new 2,1,3-benzothiadiazole-containing D–A compounds with different electron deficiency of acceptor block. The method is based on Suzuki cross-coupling and nucleophilic fluorine substitution reaction with cyano group affording the target molecules in good to excellent yields. The photophysical properties of all synthesized compounds and the working characteristics of OLEDs fabricated on their basis have been examined. Electrochemical studies have shown that the introduction of two fluorine atoms into Bz acceptor unite does not effect on the LUMO energy however leads to decrease of the HOMO energy at 0.15 eV that resulted in blue shift of the emission compared with unsubstituted compound DABzH. At the same time, the incorporation of two cyano groups leads to considerable decrease of the LUMO energy and red shift of emission band. For all synthesized compounds, we have demonstrated a feasibility of their potential utilization as emissive layers in OLED devices. The emission range of OLED changed from green to orange and red light with a saturated emission color in accordance with substituents nature in the Bz moiety. It should be noted that photoluminescence quantum yields of the synthesized compounds affect the OLED operation to a lesser degree than the electrical processes in the device.

This work was supported by the Russian Foundation for Basic Research (grant no. 19-29-08038). NMR studies and spectral characterization were performed using the equipment of Center for Molecular Composition Studies of INEOS RAS with the financial support from the Ministry of Science and Higher Education of the Russian Federation (Contract/agreement no. 075-03-2023-642). Part of this study, dedicated to the measurement of charge carriers mobility, was supported by a federal contract of IPCE RAS (grant no. 122011300052-1).

*Online Supplementary Materials*

Supplementary data associated with this article can be found in the online version at doi: 10.1016/j.mencom.2023.09.035.

## References

1 T. S. Sukhikh, D. S. Ogienko, D. A. Bashirov and S. N. Konchenko, *Russ. Chem. Bull.*, 2019, **68**, 651.

2 (*a*) C. D. Müller, A. Falcou, N. Reckefuss, M. Rojahn, V. Wiederhirn, P. Rudati, H. Frohne, O. Nuyken, H. Becker and K. Meerholz, *Nature*, 2003, **421**, 829; (*b*) S. Kato, T. Matsumoto, M. Shigeiwa, H. Gorohmaru, S. Maeda, T. Ishi-i and S. Mataka, *Chem. – Eur. J.*, 2006, **12**, 2303.

3 (*a*) H. N. Tsao, D. M. Cho, I. Park, M. R. Hansen, A. Mavrinskiy, D. Y. Yoon, R. Graf, W. Pisula, H. W. Spiess and K. Müllen, *J. Am. Chem. Soc.*, 2011, **133**, 2605; (*b*) M. Zhang, H. N. Tsao, W. Pisula, C. Yang, A. K. Mishra and K. Müllen, *J. Am. Chem. Soc.*, 2007, **129**, 3472; (*c*) P. Sonar, S. P. Singh, Y. Li, M. S. Soh and A. Dodabalapur, *Adv. Mater.*, 2010, **22**, 5409.

4 (*a*) M. Velusamy, K. R. J. Thomas, J. T. Lin, Y.-C. Hsu and K.-C. Ho, *Org. Lett.*, 2005, **7**, 1899; (*b*) W. Zhu, Y. Wu, S. Wang, W. Li, X. Li, J Chen, Z.-S. Wang and H. Tian, *Adv. Funct. Mater.*, 2011, **21**, 756; (*c*) Y. Li, *Acc. Chem. Res.*, 2012, **45**, 723; (*d*) J. Du, M. C. Biewer and M. C. Stefan, *J. Mater. Chem. A*, 2016, **4**, 15771; (*e*) Q. Liu, H. Zhan, C.-L. Ho, F.-R. Dai, Y. Fu, Z. Xie, L. Wang, J.-H. Li, F. Yan, S.-P. Huang and W.-Y. Wong, *Chem. – Asian J.*, 2013, **8**, 1892.

5 B. Patrizi, A. Iagatti, L. Abbondanza, L. Bussotti, S. Zanardi, M. Salvalaggio, R. Fusco and P. Foggi, *J. Phys. Chem. C*, 2019, **123**, 5840.

6 (*a*) J. Guo, S. Wang, N. Dai, Y. N. Teo and E. T. Kool, *PNAS*, 2011, **108**, 3493; (*b*) B. A. D. Neto, P. H. P. R. Carvalho and J. R. Correa, *Acc. Chem. Res.*, 2015, **48**, 1560.

7 (*a*) C. B. Nielsen, A. J. P. White and I. McCulloch, *J. Org. Chem.*, 2015, **80**, 5045; (*b*) W. T. Neo, K. H. Ong, T. T. Lin, S.-J. Chua and J. Xu, *J. Mater. Chem. C*, 2015, **3**, 5589; (*c*) D. Çakal, Y. E. Ercan, A. M. Önal and A. Cihaner, *Dyes Pigm.*, 2020, **182**, 108622; (*d*) A. C. Stuart, J. R. Tumbleston, H. Zhou, W. Li, S. Liu, H. Ade and W. You, *J. Am. Chem. Soc.*, 2013, **135**, 1806; (*e*) F. Babudri, G. M. Farinola, F. Naso and R. Ragni, *Chem. Commun.*, 2007, 1003; (*f*) T.-L. Wang, C.-H. Yang and Y.-Y. Chuang, *RSC Adv.*, 2016, **6**, 47676; (*g*) B. Ding, G. Kim, Y. Kim, F. D. Eisner, E. Gutiérrez-Fernández, J. Martin, M.-H. Yoon and M. Heeney, *Angew. Chem., Int. Ed.*, 2021, **60**, 19679.

8 (*a*) Y. Qiao, Y. Guo, C. Yu, F. Zhang, W. Xu, Y. Liu and D. Zhu, *J. Am. Chem. Soc.*, 2012, **134**, 4084; (*b*) L. Ren, D. Yuan, E. Gann, Y. Guo, L. Thomsen, C. R. McNeill, C.-A. Di, Y. Yi, X. Zhu and D. Zhu, *Chem. Mater.*, 2017, **29**, 4999.

9 J. Wudarczyk, G. Papamokos, V. Margaritis, D. Schollmeyer, F. Hinkel, M. Baumgarten, G. Floudas and K. Müllen, *Angew. Chem., Int. Ed.*, 2016, **55**, 3220.

10 (*a*) B. Carsten, J. M. Szarko, H. J. Son, W. Wang, L. Lu, F. He, B. S. Rolczynski, S. J. Lou, L. X. Chen and L. Yu, *J. Am. Chem. Soc.*, 2011, **133**, 20468; (*b*) H.-H. Cho, S. Kim, T. Kim, V. G. Sree, S.-H. Jin, F. S. Kim and B. J. Kim, *Adv. Energy Mater.*, 2018, **8**, 1701436.

11 J. Kumsampao, C. Chaiwai, P. Chasing, T. Chawanpunyawat, S. Namuangruk, T. Sudyoadsuk and V. Promarak, *Chem. – Asian J.*, 2020, **15**, 3029.

12 (*a*) P. S. Gribanov, D. A. Lypenko, A. V. Dmitriev, S. I. Pozin, M. A. Topchiy, A. F. Asachenko, D. A. Loginov and S. N. Osipov, *Mendeleev Commun.*, 2021, **31**, 33; (*b*) P. S. Gribanov, D. A. Loginov, D. A. Lypenko, A. V. Dmitriev, S. I. Pozin, A. E. Aleksandrov, A. R. Tameev, I. L. Martynov, A. Yu. Chernyadyev and S. N. Osipov, *Molecules*, 2021, **26**, 7596; (*c*) P. S. Gribanov, D. V. Vorobyeva, S. D. Tokarev, D. A. Petropavlovskikh, D. A. Loginov, S. E. Nefedov, F. M. Dolgushin and S. N. Osipov, *Eur. J. Org. Chem.*, 2022, e202101572; (*d*) P. S. Gribanov, D. V. Vorobyeva, S. D. Tokarev, D. A. Loginov, A. A. Danshina, S. M. Masoud and S. N. Osipov, *Asian J. Org. Chem.*, 2022, **11**, e202200603.

13 Y. Miao, X. Du, H. Wang, H. Liu, H. Jia, B. Xu, Y. Hao, X. Liu, W. Li and W. Huang, *RSC Adv.*, 2015, **5**, 4261.

14 B. S. Kim and J. Y. Lee, *Adv. Funct. Mater.*, 2014, **24**, 3970.

15 (*a*) O. Bezvikonnyi, D. Gudeika, D. Volyniuk, M. Rutkis and J. V. Grazulevicius, *Dyes Pigm.*, 2020, **175**, 108104; (*b*) A. Tomkeviciene, T. Bartiuk, A. Bucinskas, J. V. Grazulevicius and V. Jankauskas, *React. Funct. Polym.*, 2011, **71**, 796.

16 K.-C. Kao and W. Hwang, *Electrical Transport in Solids: With Particular Reference to Organic Semiconductors*, Pergamon Press, New York, 1981.

*Received: 16th May 2023; Com. 23/7173*